Journal of Oil Palm Research Vol. 35 (2) June 2023 p. 296-306
DOI: https://doi.org/10.21894/jopr.2022.0066
Status : Postprint (Author's version)

PECULIAR CRYSTALLISATION BEHAVIOUR OF PALM OIL DURING DRY FRACTIONATION

CREMER, G[1]; DANTHINE, S[1]; BLECKER, C[1] and GIBON, V[2]

[1] Food Science and Formulation, Gembloux Agro-Bio Tech, ULiège, Gembloux Belgium.

[2] Desmet Ballestra Group, R&D Center, Zaventem, Belgium.

ABSTRACT

Multi-step dry fractionation of palm oil generates fractions with specific physicochemical properties suitable for many food formulations. The present study addresses the pilot scale production of palm olein iodine value 56 starting from palm oil. The aim was to investigate the influence of the tri-saturated triacylglycerol content (StStSt) in palm oil on its crystallisation behaviour. Four StStSt contents were investigated: 7.0%, 7.6%, 8.2% and 9.8%, and the palm oil crystallisation was examined during a period of 240 min. Oil temperatures were recorded, and crystallisation kinetics were monitored by p-NMR; crystal morphology and polymorphic forms were characterised by optical microscopy and powder X-ray diffraction. One of the compositions (StStSt: 7.6%) was crystallising faster. All the crystallised matrices were filtered at 25°C with a membrane press filter; the olein yields, iodine values, cloud points and triacylglycerol compositions were analysed. The olein from the matrix crystallising faster showed a yield, an iodine value and a cloud point higher than expected. A more detailed HPLC analysis of this olein indicated unusual enrichment in OPP and depletion in OPO, which led to the conclusion of an unusual crystallisation behaviour at this specific composition.

Keywords: dry fractionation, palm oil, palm olein, peculiar crystallisation behaviour, tri-saturated triacylglycerols.

INTRODUCTION

Edible oils are made up of a wide variety of triacylglycerols (TAGs) with diverse fatty acid (FA) compositions, leading to complex physicochemical behaviour. TAGs can be classified according to their saturation: The tri-saturated (StStSt), the di-saturated (St_2U), the di-unsaturated (StU_2) and the tri-unsaturated (UUU). In palm oil (PO), tripalmitin (PPP), oleo-dipalmitin (P_2O), palmitodiolein (PO_2) and trilolein (OOO) are the most abundant of each class. PO crystallisation behaviour has important implications in the manufacture of many edible fatty products like margarine, spreads or shortenings.

Crystallisation operates in two steps: Nucleation followed by crystal growth. The driving force for nucleation is determined by the degree of supersaturation of the liquid. PO crystallisation has been extensively reviewed by Omar *et al.* (2015). The authors described the effect of chemical composition, crystallisation conditions and the presence of additives. They also focussed on crystallisation kinetics, thermal properties, polymorphism and recrystallisation aspects. Braipson-Danthine and Gibon(2007) reported a relationship between melting properties, polymorphism and TAG composition of PO and fractions. De Oliveira *et al.* (2014), Saberi *et al.* (2011) and Siew and Ng (1999) studied the effect of diacylglycerol (DAG) content on PO nucleation and crystal growth. Basso *et al.* (2010) and Verstringe *et al.* (2013; 2014) characterised the effects of PPP and monoglycerides (MAG) on crystal formation. Fredrick *et al.* (2008) studied the influence of MAG on the crystallisation behaviour of PO. Saadi *et al.* (2012) reported that 1,2-dipalmitoyl-3-oleoyl glycerol/ 1,3-dipalmitoyl-2-oleoyl glycerol (PPO/POP) were the major components of the primary nucleus developed during the crystallisation of PO and palm stearin

(PS) blend systems. The influence of sorbitan esters and soya lecithin in PO blends were studied by Kwamura (1980) and Miskandar *et al.* (2006; 2007). The effects of polyglycerol behenic acid esters on PO crystallization were described by Sakamoto *et al.* (2003) and of polyglycerol ester additives by Saw *et al.* (2017), using focused beam reflectance (FBRM) and differential scanning calorimetry (DSC). The influence of high-intensity ultrasound (HIU) on PO crystallisation was investigated by Fangfang *et al.* (2013) and Yubin *et al.* (2015). Hubbes *et al.* (2018) studied the crystallisation of PO-PS blends to obtain fats with higher PPP contents and PPP/OOO ratios; they showed that the global rate constant of the enriched PO increased with the addition of PPP. PO is a good candidate for dry fractionation, which was extensively reviewed by Deffense (1985), Gibon and Tirtiaux (2002), Gibon (2006; 2012), Gibon *et al.* (2009; 2020), Kellens *et al.* (2007), Mei Huey *et al.* (2015), Tong *et al.* (2021) and Zaliha *et al.* (2004).

Multi-step dry fractionation generates a large number of solid and liquid fractions with specific physico-chemical properties; it shows three steps, and three different routes that can be followed (*Figure 1*); the solid route (for PPP enrichment), the hard palm mid fraction (HPMF) route (for P_2O enrichment) and the liquid route (for PO_2/OOO enrichments). In dry fractionation, crystallisation is followed by crystal separation typically using membrane press filters. Chong *et al.* (2014a; 2014b; 2015) described technology for higher olein yield using a special cooling programme and additional steps mid-way. Deffense (2009) proposed an ultrasound seeding technique for improved crystallisation. Kuriyama *et al.* (2011) showed that the addition of polyglycerol ester additives enhances the olein yield and alters the fractions characteristics. Tong *et al*. (2021) reviewed the fractionation conditions that affect the yield and quality of the oil produced and published updates on the influence of seeding agents (DAG, hard fats, *etc.*) used in fractionation.
In industrial practice, a quantity of StStSt is classically added to palm olein, to ensure an efcient and reproducible crystal initiation for superolein production (Calliauw *et al.,* 2007a; 2007b; 2010). On the contrary, the naturally existing StStSt content of PO permits crystal initiation. In this work, the influence of the StStSt content on PO crystallisation is explored. PO was blended with PS and matrices containing variable contents of StStSt were considered. Crystallisation kinetics were established, operation yields were quantified and the quality of the olein fractions was analysed. The aim of this paper is to highlight and explain a particular crystallisation behaviour observed unexpectedly while studying the effect of StStSt on the crystallisation of PO during dry fractionation.

Figure 1. *Multi step dry fractionation of palm oil*

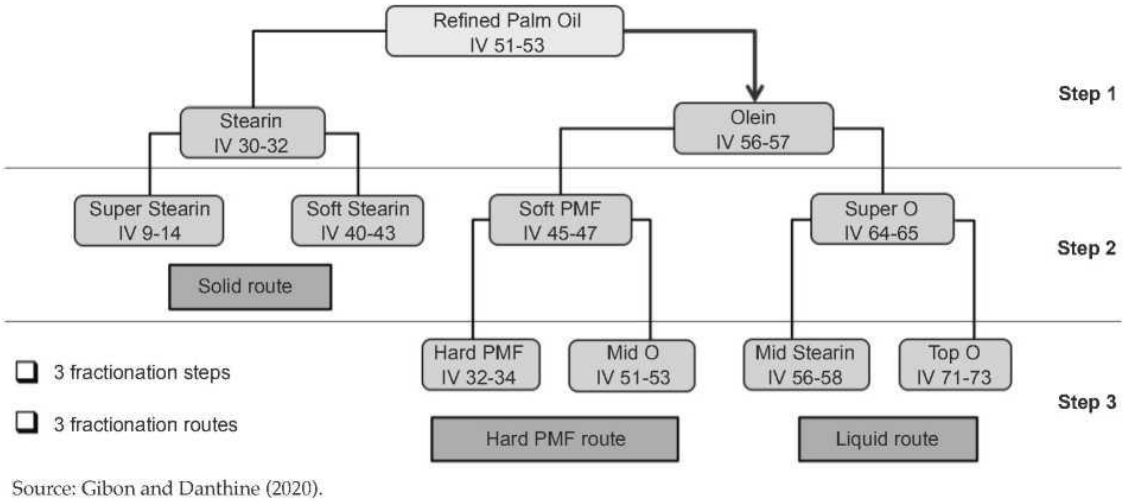

Source: Gibon and Danthine (2020).

MATERIALS AND METHODS

Materials

PO was supplied by Fuji Oil Europe (Ghent, Belgium); refined PS was provided by Desmet Ballestra Group (Zaventem, Belgium). Increasing amounts of PS were added to PO in order to reach StStSt TAGs contents of 7.0%, 7.6%, 8.2% and 9.7% in matrices named M1, M2, M3 and M4 respectively (= internal seeding). To this end, PS was first placed in an oven at 80°C to ensure a complete melting before being mixed with PO. The appropriate quantity was weighed into a preheated glass beaker and then added as liquid in the melted PO in the crystalliser

Crystallisation

Crystallisation was performed in a 30 kg capacity pilot-scale crystalliser having an exchange surface of approximately 15 m^2/T; all the tests were carried out with a total oil quantity of 20 kg. The crystalliser was a cylindrical stainless-steel double-jacketed tank connected to an external programmable water bath for controlling the temperature. The agitation was conducted by a double-bladed rotor. The oil temperature was measured by a Pt100 probe which was dipped into the oil. Cooling programmes controlling water temperature, oil temperature, and Δ oil/water temperature were applied using the Citect SCADA RunTime application (Citect, Australia). The cooling programme (13 parameters) was first optimised for each system to ensure minimal oil temperature increase during the crystal growth. The oil melting temperature was 75°C, the time allocated for crystal initiation and growth (main crystallisation) was 240 min, and the final temperature was set at 25°C (*Figure 2*). The crystallisation tests were conducted in triplicate.

Vacuum and Membrane Press Filtrations

The separation of the crystals from the liquid was done by vacuum filtrations (Büchner) and by membrane press filtrations (lab press filter). Vacuum filtrations were performed at regular intervals (every 30 min) during the main crystallisation and press filtrations were only done at the final cooling temperature (25°C).

Vacuum fltrations. Approximately 100 mL of oil were sampled from the crystalliser and immediately filtered over a Büchner (55 mm diameter) covered with filter cloth (500 L $min^{-1}.dm^{-2}$ at 196 Pa) and connected to a vacuum by means of an MZ 2C NT vacuum pump (Vacuubrand, Germany). The filtrations were stopped based on visual observation of cake dryness.

Membrane press fltrations. Press filtrations were performed with a single chamber lab-scale

membrane press filter (Choquenet S.A.S., France) covered with the same filter cloth as for vacuum filtrations. The diameter of the chamber was 5.6 cm and the width was 20 mm. The filter was filled with a volume of approximately 200 mL of oil sampled in the crystalliser (at 25°C). Air pressure, which gradually increased by 0.5 bar min^{-1} to 3 bar, was used for filling; it was then held at this value for 15 min. Afterwards, additional pressure was applied to squeeze the cake by gradually increasing the air pressure by 1 bar every 2 min to 6 bar. The squeezing pressure was held at this value for 10 min. The olein was collected in vessels and the stearin cake was recovered after opening the filter. The operation yield was derived from weighing the recovered fractions.

Monitoring of the Crystallisation by Pulsed Nuclear Magnetic Resonance (pNMR)

The kinetics of crystallisation was established by measuring the solid fat content (SFC) of the crystallising oil as a function of the time using p-NMR (Minispec-mq20, Germany). Daily calibrations were performed with three standards containing 0.0%, 31.1% and 74.8% of solids, respectively. NMR tubes were filled with crystal slurry directly from the crystalliser using a glass tube with a tight-fitting plunger (Danthine *et al.*, 2003 and Danthine, 2012) and the SFC was immediately measured.

Figure 2. *Schematic cooling curve with fast cooling crystal initiation crystal growth and final cooling steps*

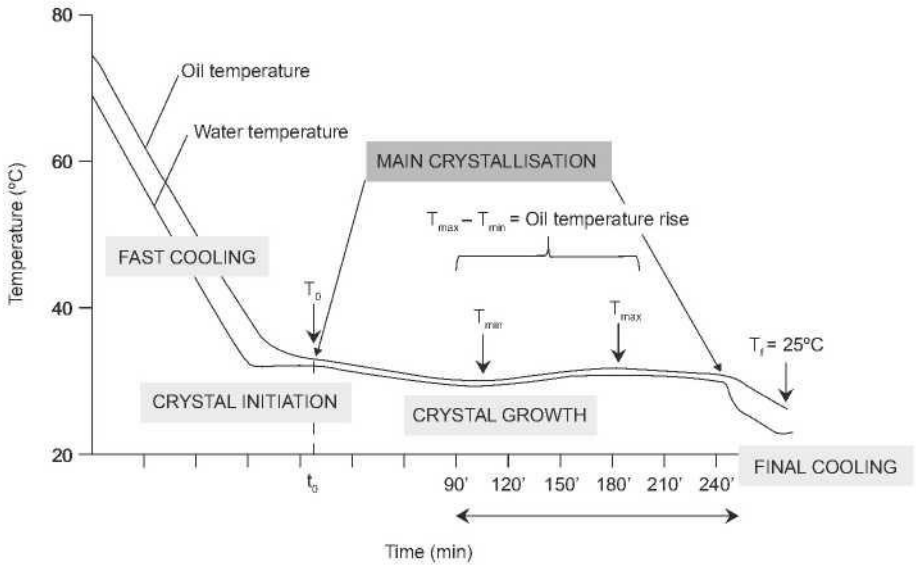

Microstructure by Optical Microscopy

For each sampling, crystal microstructure was observed by optical microscopy (OM) using a microscope coupled to a camera transmitting live images to a computer. The crystals were observed using an Eclipse E400 microscope (Nikon, Japan) equipped with a DS-Fi2 camera (Nikon, Japan).

The pictures were processed using NIS-elements 4.30 software (Nikon, Japan). A magnification of 20x was selected to analyse the pictures. One droplet of crystal slurry was randomly sampled from the NMR tube with a glass Pasteur pipette; it was then put on a microscope slide. A cover slip was carefully placed and centred over the drop of the sample to ensure homogeneity of the sample thickness. For each sampling, images of crystal microstructures were taken in triplicate.

Polymorphism by Powder X-ray Diffraction (XRD)

The polymorphic forms of the crystals were determined by XRD using a Bruker D8-Advance Diffractometer and a Lynx-eye detector (Bruker, Germany) (λ Cu= 1.5406, 40kV, 30mA). Calibration was performed using corundum, silver behenate, and tristearin standards. The X-ray diffraction patterns were analysed using DIFFRAC.EVA V4.2.2 software (Bruker, Germany). Crystals were placed on a sample holder directly after the vacuum filtration and immediately analysed. Small-angle X-ray diffraction patterns (long spacings) were investigated from 2θ = 1° to 10° with 452 steps and a time per step of 0.2 s. Wide-angle X-ray diffraction patterns (short spacings) were investigated from 2θ = 15° to 27° with 603 steps and at 0.5 s per step. The total duration of a run was approximately 7 min.

Composition by Reversed-Phase High-performance Liquid Chromatography (RP-HPLC)

The DAG content and the TAG composition were analysed by RP-HLPC based on the ofcial AOCS Ce 5b-89 method (AOCS, 2017), which does not distinguish between positional isomers. Analyses were performed with a Waters e2695 HPLC system (Waters, USA), equipped with two stainless steel Nova-Pak C18 columns (4 µm, 3.9 × 150 mm). The mobile phase was an isocratic solvent [mixture of acetone and acetonitrile (62.5/37.5 v/v)] with a flow rate of 1.2 mL min^{-1}; the injection volume was 20 µL. The samples were dissolved in methanol/chloroform (1/1 v/v) and a differential refractometer was used for the detection. The assignment was confirmed by comparing retention times with those of some standards. Peaks were integrated with Empower Pro ”Apex Track” algorithm (Waters, USA); peak areas below 4000 area counts (equivalent to approximately 0.04% of the total peak area) were not considered. The mean of two independent measurements is reported.

IodineValue(IV)byTitration

The IV was determined by titration based on the official method AOCS Cd 1d-92 (Wijs method) (AOCS, 2017). The mean of two measurements is reported.

Cloud Point (CP) by Differential Scanning Calorimetry (DSC)

DSC analyses were carried out using a Q-2000 DSC (TA Instruments, USA) coupled with a refrigerated cooling system (TA Instruments, USA), using aluminium hermetic pans. Calibration was made with indium (melting point 156.6°C; ΔH = 28.7 J g^{-1}) and eicosane (melting point 36.8°C; ΔH = 247.4 J g^{-1}) standards. Nitrogen was used as a purge gas to prevent condensation in the cells. Samples (8-10 mg) were hermetically sealed in aluminium pans; an empty pan was used as a reference.
The crystallisation onset temperatures of the four matrices (M1, M2, M3 and M4) were determined as the intersection of the baseline with the absolute highest tangent of the first crystallisation exotherm. The following time-temperature program was applied: (1) heating to 80°C at 15°C min^{-1} and holding for 10 min to erase the thermal memory, (2) cooling at -0.5°C min^{-1} to -60°C. This cooling rate of 0.5°C min^{-1} was used to mimic the slow cooling conditions used during fractionation.
The CP of the different olein obtained after filtration was determined as the intersection of the baseline with the absolute highest tangent of the first crystallisation exotherm, according to the following time-temperature program: (1) heating to 80°C at 15°C min^{-1} and holding for 10 min at 80°C to erase the thermal memory, (2) cooling to 30°C at -25°C min^{-1}, holding this temperature for 2 min and finally cooling down to -25°C at a rate of -3°C min^{-1}. All DSC measurements were done in triplicate.

Positional Isomerism by Silver Ion Highperformance Liquid Chromatography - Mass spectroscopy (Ag-HPLC-MS)

The positional isomerism of some TAGs from selected olein was determined by Ag-HPLC-MS, as described by Santoro *et al.* (2018). This separation technique uses columns where silver ions are bound to the stationary phase and rely on the ability of the π electrons of unsaturated fatty acids to react with silver ions to form polar complexes. The separation system was an HPLC Ultimate 3000 (Thermo Fisher Scientific, Italy) interfaced through an APCI ionisation source to a linear ion trap coupled to a high-resolution mass analyser (LTQ-Orbitrap Thermo Fisher Scientific, Italy). The ionisation source was heated at 450°C and used in positive ions mode. The instrument was equipped with a silver-modified cation exchange column (Luna SCX, Phenomenex, 150 × 2.0 mm, 5 µm, 100 Å). A gradient separation made up of two isocratic steps at different mobile phase compositions (*n*-heptane:ethylacetate
93:7 and 90:10) was used. The flow rate was 0.300 mL min^{-1}, and the injection volume was 10.0 µL. The mean of two measurements is reported.

Statistical Analyses

Data were statistically analysed using Minitab 19 software (Minitab LLC, USA). All assays were conducted in triplicate unless otherwise specified. Means and standard deviations were calculated and differences between means were determined with a significance level of α=0.05.

RESULTS AND DISCUSSION

Compositional properties by HPLC, IVs by titration and crystallisation onsets by DSC of the 4 matrices are listed in *Table 1*. The major StStSt TAG was PPP, followed by P_2S (S: stearic acid); the StStSt content increased gradually from 7.0% in M1 to 9.8% in M4. On the contrary, the DAG content was slightly reduced from 9.3% to 8.9% due to the lower DAG content in the stearin. The IV decreased from 52.1 to 49.9. The crystallisation onset shifted towards higher temperatures; this shift could only be attributed to the nucleation effect of higher amounts of StStSt in the matrices.
The crystallisation behaviour of PO was investigated during pilot scale dry fractionation. A water-cooling program was applied, and the oil temperature response was recorded. The crystallised oil was sampled at regular intervals and the SFC was immediately measured by p-NMR; this gave an insight into the rate of crystallisation in the

different matrices. At the same time, a microstructural analysis was performed by optical microscopy. Vacuum filtrations were carried out to recover the olein, the composition of which was determined by HPLC, and the polymorphism of the crystals by powder X-ray diffraction. *Figure 2* represents the cooling curves, with water and oil temperatures plotted as a function of time. After fast cooling, the oil was brought into supercooling conditions for crystal initiation and the crystal growth was examined for 240 min. This period was called "main crystallisation". T_0 was the oil temperature at the beginning of the main crystallisation step. Due to crystallisation exothermicity, some heat was released during the crystal growth. When this heat released by crystallisation exceeded the heat of dissipation capacity of the crystalliser, a rise in oil temperature was observed. T_{max} and T_{min} corresponded to the minimum and maximum oil temperatures observed during the crystal growth respectively. After 240 min of main crystallisation, the oil was cooled down to 25°C (T_f) before proceeding to membrane press filtration.

Figure3a shows the oil temperature rise (T_{max} - T_{min}) during the main crystallisation for the four matrices. This temperature rise was particularly important for M3 and M4 having the highest StStSt contents. A sharp increase was observed between M2 and M3 and the highest value was detected for M4 (≈1.8°C). *Figure 3b* illustrates the minimum oil temperature achieved during the main crystallisation before the rise (T_{min}); this temperature increased with the StStSt content, sharply from M1 to M2, and then gradually from M2 to M4. The ΔT_{min} between M1 and M4 was ~5°C. The time before the oil temperature rise was also determined (*Figure 3c*); it was significantly shorter for M2, M3 and M4 compared to M1 (*p*-values <0.05), and M2 had the highest reduction (40 min). In all cases, the crystallisation exothermicity caused a rise in oil temperature during the crystal growth. This rise was more important and occurred at higher temperatures in the matrices with higher StStSt content. It led to partial crystal melting, affecting the crystal slurry quality, especially for M3 and M4. The time before the temperature rise was shorter for higher StStSt contents but surprisingly, M2 showed the shortest time tending to indicate a faster crystal initiation.

Figure 4a presents the SFC of the crystallising oils determined by p-NMR as a function of time during the main crystallisation where M3 and M4 crystallised faster than M1. However, their crystallisation kinetics slowed down starting at 180 min. Interestingly, M2 presented the highest SFC from 90 min, reaching a plateau after 150 min. The final SFC after 240 min was similar (~ 9%) for all the matrices. The crystallising oil was filtered under vacuum every 30 min, and the composition of the collected olein was evaluated by RP- HPLC. The residual StStSt content in the olein is shown in *Figure 4b*. This content was higher in M3 and M4 oleins, in relation to the higher content in the initial matrices. However, the residual content in M2 olein was lower than in M1 olein after 90 min.

Polymorphism of the crystals was evaluated every 30 min during the main crystallisation. M1 and M2 showed β' polymorphism during the main crystallisation time, with WAXD peaks at 4.3 Å, 4.2 Å, 4.0 Å and 3.8 Å (*Figure 5*). In both cases, a double-chain length packing was observed (β'-2L). M3 started to crystallise in β'-2L as well but a β form was observed after 210 min, with WAXD peaks at 3.9 Å and 4.6 Å. The β form also corresponded to double chain length packing. The appearance of this β-2 form was accompanied by a slight decrease in the intensity of the β'-2L peaks. The same was seen for M4 with the β-2 peaks appearing already after 180 min. This β form most probably resulted from re-crystallisation of partially melted β'-2L crystals.

Crystal morphology was observed by optical microscopy, and the differences observed are illustrated in *Figure 6a*. After 90 min of crystallisation, bigger crystals were formed in M3 and M4, which are the matrices with higher StStSt content (≈ 150-250 µm, compared to 50-150 µm for M1 and M2). M1 showed aggregates with cauliflower-like morphology, growing from 90 to 240 min. After 240 min, M2 presented a particular morphology with aggregates made of small round-shaped structures and well-defined smaller urchin-like shaped crystals (≈ 25-50 µm) growing on the external surface (see arrows in *Figure 6b*). Very small crystals were also visible in the bulk. M3 and especially M4 crystals were more dislocated in consequence of the partial crystal melting as previously mentioned. Crystal size of M3 did not change over time (150-250 µm). However, a less dense layer was observed on crystal surface, due to re-crystallisation of the liquid phase in β-2L arising from partial melting of β'-2L crystals. A much more disaggregated structure was observed for M4, but still with this less dense layer on the crystal surface (β crystals on the surface of the β' ones).

Membrane press filtrations were carried out at 25°C (final cooling temperature). The olein yields were calculated based on the collected stearin and olein fractions. Results are presented in *Figure 7a*. The increase in StStSt content is associated with a decrease in olein yield; a Δyield of ≈ -12% is observed between M1 and M4. M3 (73.0 ± 1.6%) and M4 (64.2 ± 0.9%) matrices have significantly lower olein yield compared to M1 (76.1 ± 0.5%) (*p*-value = 0.0304, and 0.0001 respectively). The same is expected for M2 but this is not the case; the olein yield is even slightly higher in M2, highlighting again the unexpected behaviour of this matrix. The IVs by Wijs and cloud point by DSC of the oleins are presented in *Figures 7b* and *7c*. Oleins from M3 and M4 had higher IV which correlated

to lower yield. The IV of M2 olein was the highest and was significantly higher compared to M1 olein (*p*-value=0.0017). In general, oleins with a higher IV are characterised by a lower CP. This is not the case for M2 olein, which has the highest CP while having a higher IV.

The olein compositions were analysed by RPHPLC; the StStSt, St2U, StU2, UUU and DAG contents are presented in *Table 2*. The StStSt and DAG contents decreased from M1 to M4, whereas the unsaturated (UUU) and di-unsaturated (StU2) contents increased. However, the St2U content was weakly modified. Both DAG contents and TAG compositions were in line with normal variations of the IV and the cloud point.
M2 olein has an unusual behaviour. It combines a yield higher than expected with a higher IV and a higher CP. The RP-HPLC profiles did not show any peculiar composition associated with M2 olein. However, this technique does not allow the differentiation of positional isomers. In order to identify the reasons for the peculiar behaviour of M2 olein, oleins from M1, M2, M3 and M4 were analysed by Ag-HPLC. This technique is the most reliable for the regioisomeric separation of TAG. P_2O and PO_2, the most abundant TAGs, were highlighted and the corresponding 1,3-dipalmitoyl2-oleoyl glycerol/1-oleoyl-2,3-dipalmitoyl glycerol (POP/OPP) and 1,2-oleoyl-3-palmitoyl glycerol/1,3dioleoyl-2-dipalmitoyl glycerol (POO/OPO) contents were calculated as reported in *Figures 8a* and *8b*. The relative percentage of OPP was higher and the one of OPO lower in the olein from M2 compared to the other matrices. These differences are highly significant (*p*-values=0.0009 and 0.0002 for OPP and OPO respectively), thus confirming our hypothesis that the atypical behaviour of M2 olein arises from differences in positional isomers.

Table 1. *Tri-saturated triacylglycerol and diacylglycerol contents, iodine value (Wijs) and crystallization temperature onsets for M1, M2, M3 and M4*

	M1	**M2**	**M3**	**M4**
TAG (% HPLC)				
MP_2	05	0.5	0.5	0.5
PPP	5.1 (+/-0.1)	5.6 (+/-0.0)	6.1 (+/-0.0)	7.5 (+/-0.1)
P_2S	1.2 (+/-0.1)	1.2 (+/-0.1)	1.3 (+/-0.1)	1.5 (+/-0.1)
PS_2	0.1	0.2	0.2	0.2
SSS	0.1	0.1	0.1	0.1
Tota StStSt	7.0 (+/-0.1)	7.6 (+/-0.0)	8.2 (+/-0.0)	9.8 (+/-0.1)
DAG (% HPLC)	9.3 (+/-0.1)	9.2 (+/-0.1)	9.1 (+/-0.0)	8.9 (+/-0.1)
V (Wijs)	52.1 (+/-0.2)	51.6 (+/-0.2)	51.2 (+/-0.2)	49.9 (+/-0.2)
Crystallisation temperature onset (°C by DSC)	22.3 (+/-0.1)	25.1 (+/-0.1)	26.0 (+/-0.1)	27.7(+/-0.1)

Note: DAG: diacylglycerol – TAG: triacylglycerol – M: myristic acid - P: palmitic acid – S: stearic acid – St: saturated fatty acids

Figure 3 *(a) Oil temperature rise (T_{MAX}– T_{MIN}) (b) minimal oil temperature and (c) time before oil temperature rise during the main crystallisation for the four matrices.*

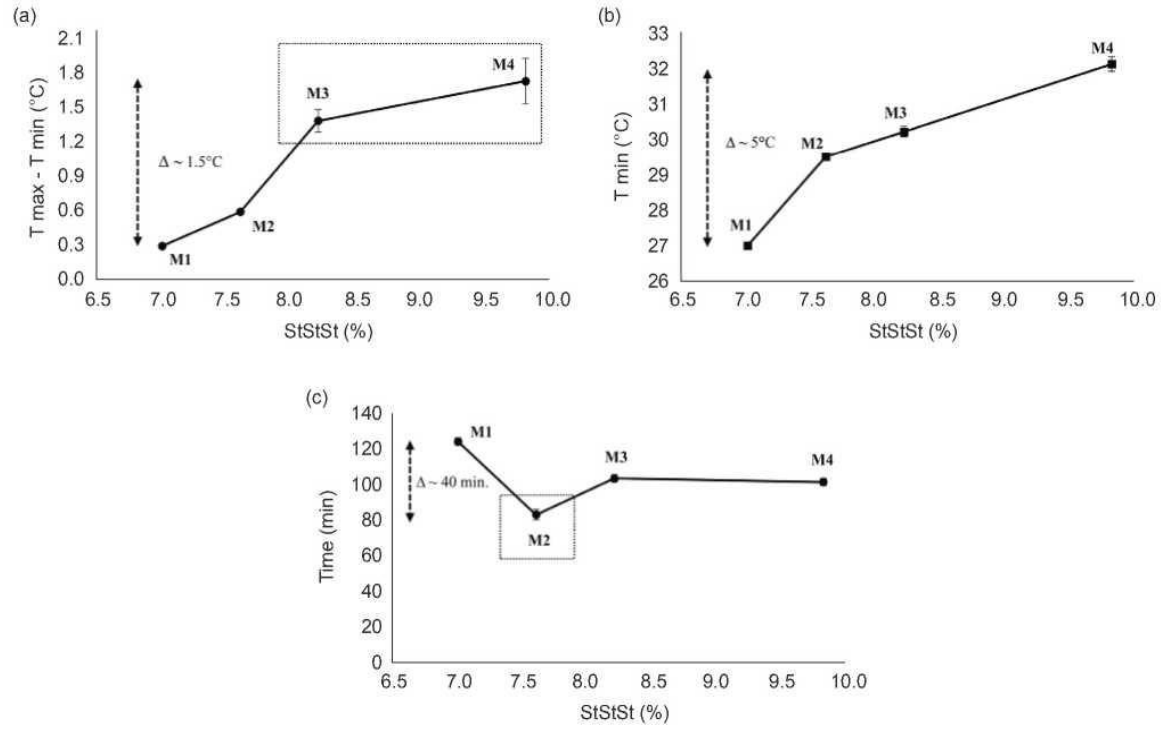

Figure 4 *(a)SFC of the crystallising oils y p-NMR and (b) StStSt content of the olein by RP-HPLC as function of the time during the main crystallisation of the four matrices.*

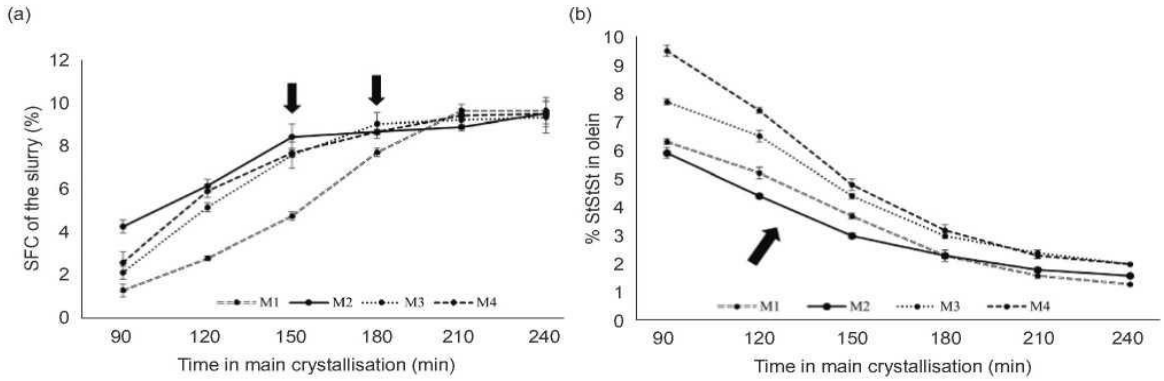

Figure 5. *Powder X-ray diffraction patterns of M1,M2, M3, and M4 crystals as function of time during the main crystallisation*

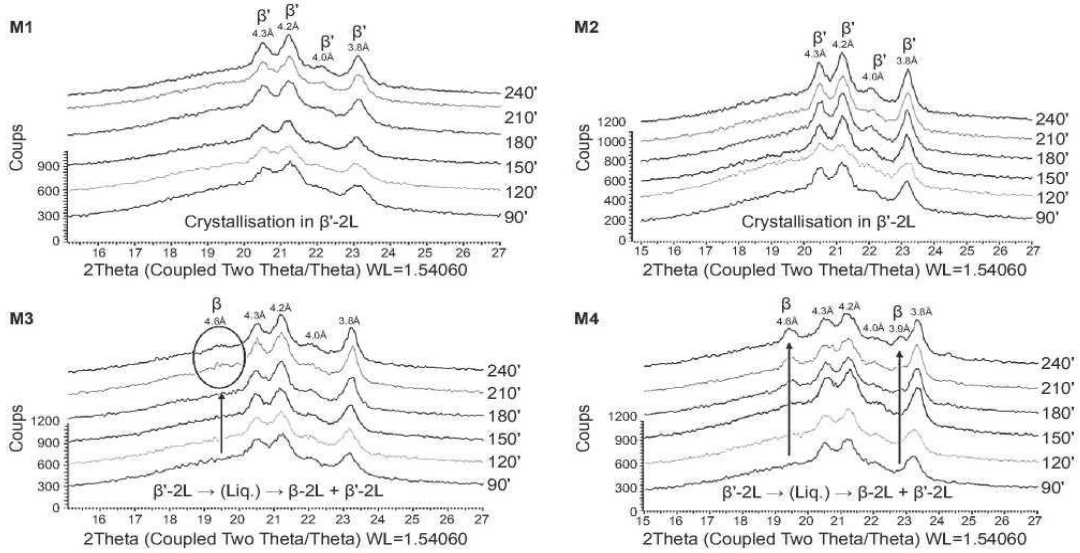

CONCLUSION

This study showed that the StStSt content in palm oil has a significant impact on crystal initiation and crystal growth. Control of the oil temperature increase was more difficult for high StStSt contents (matrices M3 and M4), inducing a partial melting of the initially formed β'-2L crystals. The resulting liquid is then further recrystallised in β-2L, leading to a mix of β' and β polymorphic forms. Although crystallising both inβ'form,M1andM2haddifferent crystal morphology. The time before temperature rise was the shortest for M2; M2 also crystallised faster than the other matrices and its StStSt content was more efficiently removed in the olein during vacuum filtrations. The highest IV and the highest cloud point as well as a higher yield than expected were observed for M2 olein after press filtration at 25°C, which is atypical behaviour. RP-HPLC could not explain this unusual behaviour; however, AgHPLC showed significantly more POP and less OPO in the M2 olein. A particular PPP/P_2O/PO_2 co-crystallisation behaviour at M2 composition explains the atypical behaviour of the M2 matrix during crystallisation to produce olein IV 56.

ACKNOWLEDGEMENT

The authors would like to thank Dr. E. Forte, R&D Manager, Soremartec Italy srl Ferrero Group, Italy and the department of molecular biotechnology and health sciences, University of Turin Italy for the silver ion HPLC analyses.

REFERENCES

AOCS (2017). Ofcial Methods and Recommended Practices of the American Oil Chemist's Society. 7th edition. Champaign, AOCS Press.

Basso, R C; Ribeiro, A P B; Masuchi, M H; Gioielli, L A; Goncalvez, L A G; Dos Santos, A O; Cardoso, L P and Grimaldi, R (2010). Tripalmitin and monoacylglycerols as modifiers in the crystallization of palm oil. *Food Chem.*, *122(4)*: 1185-1192.

Braipson-Danthine, S and Gibon, V (2007). Comparative analysis of melting properties, polymorphic behavior and triacylglycerol composition of palm oil and fractions. *Eur. J. Lipid Sci. Technol.*, *109(4)*: 359-372.

Calliauw, G; Gibon, V; De Greyt, W; Plees, L; Foubert, I and Dewettinck, K (2007a). Phase composition during palm olein fractionation and its effect on soft PMF and superolein quality. *J. Am. Oil Chem. Soc.*, *84*: 885-891.

Calliauw, G; Gibon, V and De Greyt, W (2007b). Principles of palm olein fractionation:Abit of science behind the technology. *Lipid Technol.*, *19(7)*: 152-155.

Calliauw, G; Fredrick, E; Gibon, V; De Greyt, W; Wouters, J; Foubert, I and Dewettinck, K (2010). On the fractional crystallization of palm olein: Solid solutions and eutectic solidification. *Food Res. Int.*, *43(4)*: 972-981.

Chong, C L and Yeoh, C B (2014a). Process for fractionating refined triglyceride oil. *US Patent*, US8791283B1.

Chong, C L and Yeoh, C B (2014b). Process for fractionating crude triglyceride oil. *US Patent*, US8962874B2.

Chong, C L and Yeoh, C B (2015). Offer for technology adoption of MPOB modified fractionation programme for increased olein yield. *Palm Oil Development*, *60*: 24-27.

Danthine, S and Deroanne, C (2003). Physical and textural characteristics of hydrogenated low-erucic acid rapeseed oil and low-erucic acid rapeseed oil blends. *J. Am. Oil Chem. Soc.*, *80(2)*: 109-114.

Danthine, S (2012). Physicochemical and structural properties of compound dairy fat blends. *Food Res. Int., 48(1)*: 187-195.

Deffense, E (1985). Fractionation of palm oil. *J. Am. Oil Chem. Soc*., *62(2)*: 376-385.

Deffense, E (2009). Method for continuous crystallisation with seeding for body fat. *European Patent*, EP 2166072 A1.

De Oliveira, I F; Grimaldi, R and Gonsalves, L A G (2014). Effect of diacylglycerols on crystallization of palm oil (*Elaeis guineensis*). *Eur. J. Lipid Sci. Technol.*, *116(7)*: 904-909.

Fangfang, C; Zhang, H; Xiaoyang, S; Xingguo, W and Xuebing, X (2013). Effects of ultrasonic parameters on the crystallization behavior of palm oil. *J. Am. Oil Chem. Soc., 90*: 941-949.

Fredrick, E; Foubert, I; Van De Sype, J and Dewettinck, K (2008). Influence of monoglycerides on the crystallization behavior of palm oil. *Cryst. Growth Des., 8(6)*: 1833-1839.

Gibon, V and Tirtiaux, A (2002). Latest trends in dry fractionation. *Lipid Technol., 14(3)*: 33-36.

Gibon, V (2006). Fractionation of lipids for use in food. *Modifying Lipids for Use in Food* (Gunstone, F ed.). Woodhead Publishing Ltd,Sawston. p. 201-233.

Gibon, V; Ayala, J; Dijckmans, P; Maes, J and De Greyt, W (2009). Future prospects for palm oil refining and modifications. *OCL, 16(4)*: 193-200.

Gibon, V (2012). Palm oil and palm kernel oil refining and fractionation technology. *Palm Oil: Production, Processing, Characterization and Uses*. Elsevier Inc., Netherlands. p. 329-375.

Gibon, V and Danthine, S (2020). Systematic investigation of co-crystallization properties in binary and ternary mixtures of triacylglycerols containing palmitic and oleic acids in relation with palm oil dry fractionation. *Foods*, *9(12)*: 1891.

Hubbes, S S; Danzl, W and Foerst, P (2018). Crystallization kinetics of palm oil of different geographic origins and blends thereof by the application of the Avrami model. *LWT*, *93*: 189-196.

Kellens, M; Gibon, V; Hendrix, M and De Greyt, W (2007). Dry fractionation of palm oil. *Eur. J. Lipid Sci. Technol.*, *109(4)*: 336-349.

Kuriyama, J; Miyaji, Y; Tamura, K; Zaliha, O and Chong, C L (2011). Improved sustainable fractionation of palm oil using polyglycerol fatty acid esters. *J. Oil Palm Res.*, *23*: 1141-1145.

Kwamura, K (1980). The DSC thermal analysis of crystallization behaviour of palm oil. *J. Am. Oil Chem. Soc., 56(8)*: 48-52.

Mei Huey, S; Chiew Let, C and Chee Beng Yeoh (2015). New developments in palm oil fractionation. *Palm Oil Developments, 62*: 1-7.

Miskandar, M S; Che Man, Y B; Yusoff, M S A and Abdul, R R (2006). Effect of emulsifiers on crystallization properties of low melting blends of palm oil and olein. *J. Food Lipids*, *13(1)*: 57-72.

Miskandar, M S; Che Man, Y B; Yusoff, M S A and Abdul, R R (2007). Effect of emulsifiers on crystal behaviour of palm oil blends on slow crystallization. *J. Food Lipids*, *14(1)*: 1-18.

Omar, Z; Hishamuddin, E; Sahri, M M; Fauzi, S H; Habi Mat Dian, N L; Ramli, M R and Rashid,

N A (2015). Palm oil crystallization: A review. *J. Oil Palm Res.*, *27(2)*: 97-106.

Saadi, S; Arifn, A A; Mohd Ghazali, H; Miskandar, M H; Boo, H C and Abdul Karim, S M (2012).

Application of differential scanning calorimetry (DSC), HPLC and pNMR for interpretation of primary crystallization caused by combined low and high melting TAG. *Food Chem.*, *132(1)*: 603-612.

Saberi, A H; Lai, O M and Toro-Vazquez, J F (2011). Crystallization kinetics of palm oil in blends with palm-based diacylglycerols. *Food Res. Int.*, *44(1)*: 425-435.

Sakamoto, M; Maruo, K; Kuryama, J; Kouno, M; Ueno, S and Sato, K (2003). Effects of adding polyglycerol behenic acid esters on the crystallization of palm oil. *J. Oleo. Sci*., *52(12)*: 639-645.

Santoro, V; Dal Bello, F; Aigotti, R; Gastaldi, D; Romaniello, F; Forte, E; Magni, M; Baiocchi, C and Medana, C (2018). Characterization and determination of interesterification markers (Triacylglycerol Regioisomers) in confectionery oils by liquid chromatography-mass spectrometry. *Foods, 7(2)*: 23.

Saw, M H; Hishamuddin, E; Chong, C L; Yeoh, C B and Lim, W H (2017). Effect of polyglycerol esters additive on palm oil crystallization using focused beam reflectance measurement and differential scanning calorimetry. *Food Chem.*, *214*: 277-284.

Siew and Ng (1999). Influence of diglycerides on crystallization of palm oil. *J. Sci. Food Agric.*, *79(5)*: 722-726.

Tong, S C; Tang, T K and Lee, Y Y (2021). A review on the fundamentals of palm oil fractionation:

Processing conditions and seeding agents.*Eur. J. Lipid Sci. Technol.*, *123(12)*: 2100132.

Verstringe, S; Danthine, S; Blecker, C; Depypere, F and Dewettinck, K (2013). Influence of monopalmitin in the isothermal crystallization mechanism of palm oil. *Food Res. Int.*, *51(1)*:344-353.

Verstringe, S; Danthine, S; Blecker, C and Dewettinck, K (2014). Influence of commercial monoacylglycerols on the crystallization mechanism of palm oil as compared to its pure constituants. *Food Res. Int.*, *62*: 694-700.

Yubin, Y and Martini, S (2015). Application of highintensity ultrasound to palm oil in a continuous system. *J. Agric. Food Chem., 63(1)*: 319-327.

Zaliha, O; Chong, C L; Cheow, C S; Norizzah, A R and Kellens, M J (2004). Crystallization properties of palm oil by dry fractionation. *Food Chem., 86(2)*: 245-250.